Available online www.worldscientificnews.com

World Scientific News

An International Scientific Journal

WSN 208 (2025) 126-143 EISSN 2392-2192

# On the Heat Transfer Analysis in a Convective-Radiative Porous Fin under the Influence of Magnetic Field: Application of Homotopy Analysis and Differential Transformation Methods

**Gbeminiyi Sobamowo[1], Lawrence Jayesimi[2], Olanrewaju Isiaq[3], Carlos Agbelusi[4]**

[1,4]Department of Mechanical Engineering, University of Lagos, Nigeria

[2] Works and Physical Planning Department, University of Lagos, Nigeria

[3]Department of Mechanical Engineering, Yaba College of Technology, Yaba, Lagos, Nigeria

**ABSTRACT**

In this work, homotopy analysis and differential transformation methods are applied to study the thermal performance of magnetohydrodynamic convective-radiative porous fin with temperature-invariant thermal conductivity. Also, the effects of other parameters of the thermal model parameters on the heat transfer behaviour of the extended surface are analytically investigated. The results show that as the inclination of fin, convective, radiative, magnetic, and porous parameters increase, the adimensional fin temperature decreases, which leads to an increase in the heat transfer rate through the fin and the thermal efficiency of the porous fin. It is established that the porous fin is more efficient and effective for low values of convective, radiative, magnetic, and porous parameters. Apart from the fact that the work demonstrates the ease of application of the two methods, it is hoped that study will help in proper thermal analysis of fins and in the design of passive heat enhancement devices used for thermal and electronic systems.

***Keywords:*** Magnetic field, Convective-radiative fin, Thermal Performance, homotopy analysis method, differential transformation method.

(Received 21 August 2025; Accepted 18 September 2025; Date of Publication 7 October 2025)

## 1. INTRODUCTION

The various applications of fins as passive cooling devices can be seen in thermal and electronics systems. Although, solid fins have been applied avoid thermal damage or enhance thermal control of the thermal and electronics equipment, further heat transfer enhancement has been achieved through the use of porous fins. The importance of such fins in various thermal and electronic equipment aroused various studies. In these studies, Kiwan and Al-Nimir [1] pointed out use of fins with pores for thermal augumentation of the extended surfaces. Gong et al.[2] analyzed the perfomance of porous heat sink in micro-channel. Ali et al. [3] studied the infleunce of fin heat sink geometry on the thermal management of electronics. In an ealier work. Saedodin [4] explored the heat transfer in fin with pores under natural convection condition. Oguntala et al. [5] examined the impacts of particles deposition on thermal performance of a convective-radiative porous fin. In another work, Sobamowo et al. [6] also presented a study the performance of aporous fin under natural convection condition. However, the effects of temperature-dependent thermal conductivity and internal heat generation was also considered in their work. A study on transient heat transfer analysis of fins with different fin profiles having variable thermal properties and internal heat generation was considered by Mosayebidorcheh et al. [7]. Kim and Mudawar [8] investigated the heat flow in micro-channel heat sink different geometries. With the aid of differential transformation method, Moradi et al. [9] analyzed the heat transfer in a convection-radiative triangular porous fins with variable thermal conductivity. The influence of magnetic field on a convection-radiative rectangular porous fins with variable thermal conductivity was investigated by Oguntala et al. [10]. Wan et al. [11] experiementally studied the fluid flow and heat transfer in a miniature porous heat sink under high heat flux application, while Naphon et al.[12] had earlier presented a numerical investigation of fluid flow and heat transfer in the mini-fin heat sink. Optimum design and thermal stability of an extended surface with variable thermal properties and internal heat generation was studied by Oguntala et al. [13] while Sobamowo [14] applied Galerkin's method of weighted residual to examine the thermal performance of rectangular fin with variable thermal properties and internal heat generation. Seyf and Feizbakhshi [15] submitted a computational study on the effects of nanofluid on the heat transfer capacity of micro-pin-fin heat sinks. Fazeli et al. [16] presented both experimental and numerical investigations of the effect of silica nanofluid on the heat transfer in a miniature heat sink.

In the above reviewed works, various analytical and numerical methods have been employed to study the heat transfer enhancement of the extended surfaces. In this present work, the ease of application and efficiency of homotopy and differential transformation methods are demonstrated to study the thermal performance of magnetohydrodynamic convective-radiative porous fin with temperature-invariant thermal conductivity. Also, the effects of other parameters of the thermal model parameters on the heat transfer behaviour of the extended surface are analytically investigated using the improved differential transformation method.

## 2. PROBLEM FORMULATION

Consider a longitudinal rectangular fin with pores having convective and radiative heat transfer, as shown in Fig. 1. In order to derive the thermal model of the porous fin, it is assumed that the porous medium is isotropic, homogeneous, and saturated with single-phase fluid. The physical and thermal properties of the fin and the surrounding fluid surface are constant. The temperature varies in the fin is only along the length of the fin, as shown in the Fig. 1. and there is a perfect contact between the fin base and the prime surface.

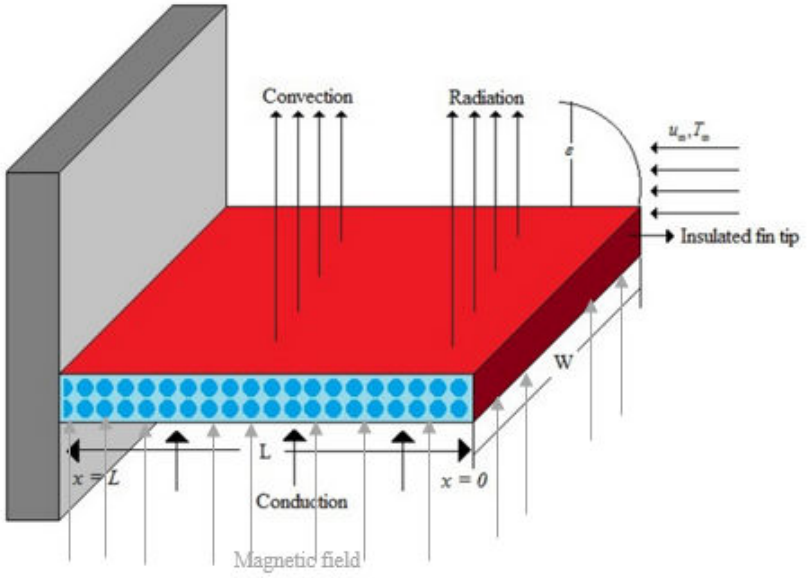


**Figure 1**. Convective-radiative longitudinal fin with pores.

From the assumptions and with the aid of Darcy's model, the energy balance is

$$q_x - \left( q_x + \frac{\delta q}{\delta x} dx \right) + q(T)\, dx = \dot{m} c_p (T - T_a) + hP(1-\varepsilon)(T - T_a)dx + \sigma \varepsilon P(T^4 - T_a^4)dx + \frac{J_c \times J_c}{\sigma} dx \tag{1}$$

The fluid flows through the pores at the rate of mass flow given as

$$\dot{m} = \rho u(x) W dx \tag{2}$$

Also, the fluid velocity is given as

$$u(x) = \frac{gK\beta_R (T - T_a)}{\nu} \tag{3}$$

Then, Equ. (1) becomes

$$q_x - \left( q_x + \frac{\delta q}{\delta x} dx \right) = \frac{\rho c_p g K \beta_p}{\nu} (T - T_a)^2 dx + hP(1-\varepsilon)(T - T_a)dx + \sigma \varepsilon P(T^4 - T_a^4)dx + \frac{J_c \times J_c}{\sigma} dx \tag{4}$$

As $dx \rightarrow 0$, Eq. (3.5) reduces

$$-\frac{dq}{dx} = \frac{\rho c_p g K \beta_p}{\nu} (T - T_a)^2 + hP(1-\varepsilon)(T - T_a) + \sigma \varepsilon P(T^4 - T_a^4) + \frac{J_c \times J_c}{\sigma} \tag{5}$$

Applying Fourier's law for the heat conduction in the solid, one has

$$q = -k_{eff} A_{cr} \frac{dT}{dx} \tag{6}$$

where the effective thermal conductivity of the fin is given as

$$k_{eff} = \phi k_f + (1-\phi) k_s \tag{7}$$

According to Roseland diffusion approximation, the radiative heat transfer rate can be written as

$$q = -\frac{4\sigma A_{cr}}{3\beta_R} \frac{dT^4}{dx} \tag{8}$$

From Eqs. (6) and (8), the total rate of heat transfer is given by

$$q = -k_{eff} A_{cr} \frac{dT}{dx} - \frac{4\sigma A_{cr}}{3\beta_R} \frac{dT^4}{dx} \tag{9}$$

Substitution of Eq. (9) into Eq. (6) leads to

$$\begin{aligned} &\frac{d}{dx}\left( k_{eff} A_{cr} \frac{dT}{dx} + \frac{4\sigma A_{cr}}{3\beta_R} \frac{dT^4}{dx} \right) = \frac{\rho c_p g K \beta_p}{v} (T - T_a)^2 \\ &+ hP(1-\varepsilon)(T - T_a) + \sigma \varepsilon P (T^4 - T_a^4) + \frac{J_c \times J_c}{\sigma} \end{aligned} \tag{10}$$

Expansion of the first term in Eq. (10), provides the governing equation for the required heat transfer

$$\begin{aligned} &\frac{d^2T}{dx^2} + \frac{4\sigma}{3\beta_R k_{eff}} \frac{d}{dx}\left( \frac{dT^4}{dx} \right) - \frac{\rho c_p g K \beta_p}{k_{eff} t v} (T - T_a)^2 \\ &- \frac{h(1-\varepsilon)}{k_{eff} t} (T - T_a) - \frac{\sigma \varepsilon}{k_{eff} t} (T^4 - T_a^4) - \frac{J_c \times J_c}{\sigma} = 0 \end{aligned} \tag{11}$$

The boundary conditions are

$$x = 0, \quad \frac{dT}{dx} = 0, \tag{12a}$$

$$x = L, \quad T = T_b \tag{12b}$$

But

$$\frac{J_c \times J_c}{\sigma} = \sigma B_o^2 u^2 \tag{13}$$

After substitution of Eq. (13) into Eq. (11), we have

$$\frac{d^2T}{dx^2} + \frac{4\sigma}{3\beta_R k_{eff}} \frac{d}{dx}\left(\frac{dT^4}{dx}\right) - \frac{\rho c_p g K \beta_p}{k_{eff} tv}(T - T_a)^2 - \frac{h(1-\varepsilon)}{k_{eff} t}(T - T_a) - \frac{\sigma\varepsilon}{k_{eff} t}(T^4 - T_a^4) - \frac{\sigma B_o^2 u^2}{k_{eff} A_{cr}}(T - T_a) = 0 \tag{14}$$

The term $T^4$ can be expressed as a linear function of temperature as

$$T^4 = T_\infty^4 + 4T_\infty^3 (T - T_\infty) + 6T_\infty^2 (T - T_\infty)^2 + \ldots \cong 4T_\infty^3 T - 3T_\infty^4 \tag{15}$$

Substitution of Eq. (13) into Eq. (11), results in

$$\frac{d^2T}{dx^2} + \frac{16\sigma}{3\beta_R k_{eff}} \frac{d^2T}{dx^2} - \frac{\rho c_p g K \beta_p}{k_{eff} tv}(T - T_a)^2 sin(\gamma) - \frac{h(1-\varepsilon)}{k_{eff} t}(T - T_a) - \frac{4\sigma\varepsilon T_a^3}{k_{eff} t}(T - T_a) - \frac{\sigma B_o^2 u^2}{k_{eff} A_{cr}}(T - T_a) = 0 \tag{16}$$

Applying the following adimensional parameters in Eq. (15) to Eq. (14),

$$X = \frac{x}{L},\ \theta = \frac{T - T_a}{T_b - T_a} \quad S_{hi} = \frac{gk\beta_p (T_b - T_\infty) L}{\alpha \nu k_r},\ Nc_i = \frac{hL}{k_{eff} t}$$

$$Rd = \frac{4\sigma_{st} T_\infty^3}{3\beta_R k_{eff}},\ Nr_i = \frac{4\sigma_{st} L T_\infty^3}{k_{eff} t},\ Ha_i = \frac{\sigma B_0^2 u^2 b}{k_{eff} A_b}. \tag{17}$$

One arrives at the adimensional form of the governing Eq. (16) as presented in Eq. (18),

$$(1 + 4Rd)\frac{d^2\theta}{dX^2} - S_{hi} sin(\gamma)\theta^2 - Nc_i(1-\varepsilon)\theta - Nr_i\theta - Ha_i\theta = 0 \tag{18}$$

and the adimensional boundary conditions

$$X = 0,\quad \frac{d\theta}{dX} = 0 \tag{19a}$$

$$X = 1,\quad \theta = 1 \tag{19b}$$

Which can be written as

$$\frac{d^2\theta}{dX^2} - S_h sin(\gamma)\theta^2 - Nc(1-\varepsilon)\theta - Nr\theta - Ha\theta = 0 \quad (20)$$

where

$$S_h = \frac{S_{hi}}{(1+4Rd)},\ Nc = \frac{Nc_i}{(1+4Rd)},\ Nr = \frac{Nr_i}{(1+4Rd)},\ Ha = \frac{Ha_i}{(1+4Rd)}$$

## 3. APPLICATION OF HOMOTOPY ANALYSIS METHOD TO THE NONLINEAR THERMAL PROBLEM

It can be seen that the above governing differential equation is highly nonlinear, and such nonlinearity imposes some difficulties in the development of exact analytical methods to generate closed form solution for the equation. Therefore, homotopy analysis method is used in this work. The homotopy analysis method (HAM) which is an analytical scheme for providing approximate solutions to the ordinary differential equations, is adopted in generating solutions to the ordinary nonlinear differential equations .Upon constructing the homotopy, the initial guess and auxiliary linear operator can be expressed as

$$\theta_0(X) = 1 \quad (21)$$

$$L(\theta) = \theta'' \quad (22)$$

$$L(c_1 X + c_2) = 0 \quad (23)$$

Where $c_i\,(i = 1,2,3,4)$ are constants. Let $P = \in [0,1]$ connotes the embedding parameter and $\hbar$ is the non-zero auxiliary parameter. Therefore, the homotopy is constructed as

### 3.1. Zeroth-order deformation equations

$$(1-p)L[\theta(X;p) - \theta_0(X)] = p\hbar H(X)N[\theta(X;p)] \quad (24)$$

$$\theta'(0;p) = 0;\ \ \theta(1;p) = 1; \quad (25)$$

when $p = 0$ and $p = 1$ we have

$$\theta(X;0) = \theta_0(X)\ ;\ \theta(X;1) = \theta(X) \quad (26)$$

As p increases from *0 to 1*. $\theta(X;p)$ varies from $\theta_o(X)$ to $\theta(X)$. By Taylor's theorem and utilizing Eq. (20), $\theta(X;p)$ can be expanded in the power series of p as follows:

$$\theta(X;p)=\theta_0(X)+\sum_{m-1}^{\infty}\theta_m(X)p^m, \qquad \theta_m(X)=\frac{1}{m!}\frac{\partial^m(\theta(X;p))}{\partial p^m}\bigg|_{p=0} \tag{27}$$

where $\hbar$ is chosen such that the series is convergent at p = 1; therefore, by Eq. (27) it is easily shown that

$$\theta(X)=\theta_0(X)+\sum_{m-1}^{\infty}\theta_m(X) \tag{28}$$

### 3.2. m-th order deformation equations

$$L[\theta_m(\eta)-\chi_m\theta_{m-1}(\eta)]=\hbar H(X)R_m(X) \tag{29}$$

$$\theta'(0;p)=0;\ \ \theta(1;p)=0; \tag{30}$$

where

$$R_m(X)=\frac{d^2\theta(X;p)}{dX^2}-S_h(sin\gamma)\sum_{i=0}^{n-1}\theta_{n-1-k}\theta_k-\left((Nc(1-\varepsilon)+Nr+Ha)\right)\theta_{n-1} \tag{31}$$

Now the results for the convergence, differential equation and the auxiliary function are determined according to the solution expression. Therefore, we assume

$$H(X)=1 \tag{32}$$

The analytic solution is developed using the MATLAB computational stencil. Hence, the first deformation is expressed below

$$\theta_1(X)=-\frac{1}{2}\hbar\left(S_h sin(\gamma)+(Nc(1-\varepsilon)+Nr+Ha)\right)X^2+\frac{1}{2}\hbar S_h sin(\gamma)+\frac{1}{2}\hbar(Nc(1-\varepsilon)+Nr+Ha) \tag{33}$$

$$\begin{aligned}\theta_2(X)=&\frac{5}{120}\hbar^2\left(-S_h sin(\gamma)-(Nc(1-\varepsilon)+Nr+Ha)\right)\left(-2S_h sin(\gamma)-(Nc(1-\varepsilon)+Nr+Ha)\right)X^4\\&+\frac{1}{2}\left[\begin{matrix}-\hbar S_h sin(\gamma)-\hbar(Nc(1-\varepsilon)+Nr+Ha)-\hbar^2 S_h sin(\gamma)-\hbar^2(Nc(1-\varepsilon)+Nr+Ha)\\-\hbar^2\left(S_h sin(\gamma)\right)^2-\frac{1}{2}\hbar^2(Nc(1-\varepsilon)+Nr+Ha)^2-\frac{3}{2}\hbar^2 S_h sin(\gamma)(Nc(1-\varepsilon)+Nr+Ha)\end{matrix}\right]X^2\\&+\frac{5}{24}\hbar^2(Nc(1-\varepsilon)+Nr+Ha)^2+\frac{5}{8}\hbar^2(Nc(1-\varepsilon)+Nr+Ha)+\frac{1}{2}\hbar(Nc(1-\varepsilon)+Nr+Ha)\\&+\frac{1}{2}\hbar^2 S_h sin(\gamma)+\frac{1}{2}\hbar^2(Nc(1-\varepsilon)+Nr+Ha)+\frac{1}{2}\hbar S_h sin(\gamma)+\frac{5}{12}\hbar^2\left(S_h sin(\gamma)\right)^2\end{aligned} \tag{34}$$

Similarly $\theta_3(\eta)$, $\theta_4(\eta)$, $\theta_5(\eta)$... are found, but they are too large expressions that cannot be included in this paper. However, they are included in the results displayed graphically. From the principle of HAM

$$\theta(X)=\theta_0(X)+\sum_{m=1}^{\infty}\theta_m(X)=\theta_0(X)+\theta_1(X)+\theta_2(X)+... \tag{35}$$

Therefore, substitute Eqs. (25), (33) and (34) into Eq. (35), we have

$$\begin{aligned}\theta(X)=&1-\frac{1}{2}\hbar\left(S_h sin(\gamma)+(Nc(1-\varepsilon)+Nr+Ha)\right)X^2+\frac{1}{2}\hbar S_h sin(\gamma)+\frac{1}{2}\hbar(Nc(1-\varepsilon)+Nr+Ha)\\&+\frac{5}{120}\hbar^2\left(-S_h sin(\gamma)-(Nc(1-\varepsilon)+Nr+Ha)\right)\left(-2S_h sin(\gamma)-(Nc(1-\varepsilon)+Nr+Ha)\right)X^4\\&+\frac{1}{2}\left[\begin{array}{l}-\hbar S_h sin(\gamma)-\hbar(Nc(1-\varepsilon)+Nr+Ha)-\hbar^2 S_h sin(\gamma)-\hbar^2(Nc(1-\varepsilon)+Nr+Ha)\\-\hbar^2\left(S_h sin(\gamma)\right)^2-\frac{1}{2}\hbar^2(Nc(1-\varepsilon)+Nr+Ha)^2-\frac{3}{2}\hbar^2 S_h sin(\gamma)(Nc(1-\varepsilon)+Nr+Ha)\end{array}\right]X^2\\&+\frac{5}{24}\hbar^2(Nc(1-\varepsilon)+Nr+Ha)^2+\frac{5}{8}\hbar^2(Nc(1-\varepsilon)+Nr+Ha)+\frac{1}{2}\hbar(Nc(1-\varepsilon)+Nr+Ha)\\&+\frac{1}{2}\hbar^2 S_h sin(\gamma)+\frac{1}{2}\hbar^2(Nc(1-\varepsilon)+Nr+Ha)+\frac{1}{2}\hbar S_h sin(\gamma)+\frac{5}{12}\hbar^2\left(S_h sin(\gamma)\right)^2+...\end{aligned} \tag{36}$$

### 3.3. Convergence of the HAM solution

In order to control the convergence rate of $\hbar$ in the approximate analytical solutions given by HAM, Liao [17] presented the auxiliary parameter. It is established that the convergence rate of approximation for the HAM solution strongly depend on the value of the auxiliary parameter. For the 10th-order of approximation, different values of the model parameters are used for the different simulations to arrive at the acceptable range of values of the parameter $\hbar$ for the difference controlling parameters of the model.

## 4. METHOD OF SOLUTION: DIFFERENTIAL TRANSFORM METHOD

The nonlinear thermal model is also solved using differential transformation method. The definition and the operational properties of the method can be found in our previous work [31]. The differential transformation of the governing differential equation in Eq. (19) is given as

$$\left(1+4Rd\right)(k+1)(k+2)\Theta(k+2)-S_h sin(\gamma)\sum_{l=0}^{k}\Theta(l)\Theta(k-l)-Nc(1-\tilde{\varepsilon})\Theta(k)-Nr\Theta(k)-Ha\Theta(k)=0 \tag{37}$$

and the boundary condition in Eq. (20)

$$k=0,\quad \theta(1)=0$$

$$\sum_{l=0}^{k}\theta(1)=1 \quad\Rightarrow\quad \theta(0)=\lambda \tag{38}$$

Eq. (37) could be further simplified as

$$\Theta(k+2)=\frac{1}{(1+4Rd)(k+1)(k+2)}\left\{S_h sin(\gamma)\sum_{l=0}^{k}\Theta(l)\Theta(k-l)+Nc(1-\tilde{\varepsilon})\Theta(k)+Nr\Theta(k)+H\Theta(k)\right\} \quad (39)$$

Which can be written as

$$\Theta(k+2)=\frac{S_h sin(\gamma)}{(k+1)(k+2)(1+4Rd)}\sum_{l=0}^{k}\left[\Theta(l)\Theta(k-l)\right]+\frac{Nc(1-\tilde{\varepsilon})+Nr+Ha}{(k+1)(k+2)(1+4Rd)}\Theta(k) \quad (40)$$

Now for the counter *k=0, 1, 2, 3..., N* in Eq. (40), we have

$$\Theta(0)=\lambda$$

$$\Theta(1)=0$$

$$\Theta(2)=\frac{1}{2}\left(\lambda^2\left(\frac{S_h sin(\gamma)}{(1+4Rd)}\right)+\lambda\left(\frac{Nc(1-\tilde{\varepsilon})+Nr+Ha}{(1+4Rd)}\right)\right)$$

$$\Theta(3)=0$$

$$\Theta(4)=\frac{1}{24}\left(2\lambda^3\left(\frac{S_h sin(\gamma)}{(1+4Rd)}\right)^2+3\lambda^2\left(\frac{S_h sin(\gamma)}{(1+4Rd)}\right)\left(\frac{Nc(1-\tilde{\varepsilon})+Nr+Ha}{(1+4Rd)}\right)+\lambda\left(\frac{Nc(1-\tilde{\varepsilon})+Nr+Ha}{(1+4Rd)}\right)^2\right)$$

$$\Theta(5)=0$$

$$\Theta(6)=\frac{1}{720}\left(\begin{array}{l}10\lambda^4\left(\frac{S_h sin(\gamma)}{(1+4Rd)}\right)^3+20\lambda^3\left(\frac{S_h sin(\gamma)}{(1+4Rd)}\right)^2\left(\frac{Nc(1-\tilde{\varepsilon})+Nr+Ha}{(1+4Rd)}\right)\\+11\lambda^2\left(\frac{S_h sin(\gamma)}{(1+4Rd)}\right)\left(\frac{Nc(1-\tilde{\varepsilon})+Nr+Ha}{(1+4Rd)}\right)^2+\lambda\left(\frac{Nc(1-\tilde{\varepsilon})+Nr+Ha}{(1+4Rd)}\right)^3\end{array}\right)$$

$$\Theta(7)=0$$

$$\Theta(8)=\frac{1}{40320}\left(\begin{array}{l}80\lambda^5\left(\frac{S_h sin(\gamma)}{(1+4Rd)}\right)^4+200\lambda^4\left(\frac{S_h sin(\gamma)}{(1+4Rd)}\right)^3\left(\frac{Nc(1-\tilde{\varepsilon})+Nr+Ha}{(1+4Rd)}\right)\\+162\lambda^3\left(\frac{S_h sin(\gamma)}{(1+4Rd)}\right)^3\left(\frac{Nc(1-\tilde{\varepsilon})+Nr+Ha}{(1+4Rd)}\right)^2\\+43\lambda^2\left(\frac{S_h sin(\gamma)}{(1+4Rd)}\right)\left(\frac{Nc(1-\tilde{\varepsilon})+Nr+Ha}{(1+4Rd)}\right)^3+\lambda\left(\frac{Nc(1-\tilde{\varepsilon})+Nr+Ha}{(1+4Rd)}\right)^4\end{array}\right)$$

$$\Theta(9)=0$$

$$\Theta(10)=\frac{1}{3628800}\left(\begin{array}{l}1000\lambda^6\left(\frac{S_h sin(\gamma)}{(1+4Rd)}\right)^5+3000\lambda^5\left(\frac{S_h sin(\gamma)}{(1+4Rd)}\right)^4\left(\frac{Nc(1-\tilde{\varepsilon})+Nr+Ha}{(1+4Rd)}\right)\\+3170\lambda^4\left(\frac{S_h sin(\gamma)}{(1+4Rd)}\right)^3\left(\frac{Nc(1-\tilde{\varepsilon})+Nr+Ha}{(1+4Rd)}\right)^2\\+1340\lambda^3\left(\frac{S_h sin(\gamma)}{(1+4Rd)}\right)^2\left(\frac{Nc(1-\tilde{\varepsilon})+Nr+Ha}{(1+4Rd)}\right)^3\\+171\lambda^2\left(\frac{S_h sin(\gamma)}{(1+4Rd)}\right)\left(\frac{Nc(1-\tilde{\varepsilon})+Nr+Ha}{(1+4Rd)}\right)^4+\lambda\left(\frac{Nc(1-\tilde{\varepsilon})+Nr+Ha}{(1+4Rd)}\right)^5\end{array}\right)$$

$$\Theta(11)=0$$

$$\Theta(12)=\frac{1}{476001600}\left(\begin{array}{l}17600\lambda^7\left(\frac{S_h sin(\gamma)}{(1+4Rd)}\right)^6+61600\lambda^6\left(\frac{S_h sin(\gamma)}{(1+4Rd)}\right)^5\left(\frac{Nc(1-\tilde{\varepsilon})+Nr+Ha}{(1+4Rd)}\right)\\+80560\lambda^5\left(\frac{S_h sin(\gamma)}{(1+4Rd)}\right)^4\left(\frac{Nc(1-\tilde{\varepsilon})+Nr+Ha}{(1+4Rd)}\right)^2\\+47400\lambda^4\left(\frac{S_h sin(\gamma)}{(1+4Rd)}\right)^3\left(\frac{Nc(1-\tilde{\varepsilon})+Nr+Ha}{(1+4Rd)}\right)^3\\+11522\lambda^3\left(\frac{S_h sin(\gamma)}{(1+4Rd)}\right)^2\left(\frac{Nc(1-\tilde{\varepsilon})+Nr+Ha}{(1+4Rd)}\right)^4\\+683\lambda^2\left(\frac{S_h sin(\gamma)}{(1+4Rd)}\right)\left(\frac{Nc(1-\tilde{\varepsilon})+Nr+Ha}{(1+4Rd)}\right)^5+\lambda\left(\frac{Nc(1-\tilde{\varepsilon})+Nr+Ha}{(1+4Rd)}\right)^6\end{array}\right)$$

$$\Theta(13)=0$$

$$\Theta(14)=\frac{1}{87178291200}\left(\begin{array}{l}418000\lambda^8\left(\frac{S_h sin(\gamma)}{(1+4Rd)}\right)^7+1672000\lambda^7\left(\frac{S_h sin(\gamma)}{(1+4Rd)}\right)^6\left(\frac{Nc(1-\tilde{\varepsilon})+Nr+Ha}{(1+4Rd)}\right)\\+2604000\lambda^6\left(\frac{S_h sin(\gamma)}{(1+4Rd)}\right)^5\left(\frac{Nc(1-\tilde{\varepsilon})+Nr+Ha}{(1+4Rd)}\right)^2+\\1960000\lambda^5\left(\frac{S_h sin(\gamma)}{(1+4Rd)}\right)^4\left(\frac{Nc(1-\tilde{\varepsilon})+Nr+Ha}{(1+4Rd)}\right)^3\\+7087300\lambda^4\left(\frac{S_h sin(\gamma)}{(1+4Rd)}\right)^3\left(\frac{Nc(1-\tilde{\varepsilon})+Nr+Ha}{(1+4Rd)}\right)^4\\+101460\lambda^3\left(\frac{S_h sin(\gamma)}{(1+4Rd)}\right)^2\left(\frac{Nc(1-\tilde{\varepsilon})+Nr+Ha}{(1+4Rd)}\right)^5+\\2731\lambda^2\left(\frac{S_h sin(\gamma)}{(1+4Rd)}\right)\left(\frac{Nc(1-\tilde{\varepsilon})+Nr+Ha}{(1+4Rd)}\right)^6+\lambda\left(\frac{Nc(1-\tilde{\varepsilon})+Nr+Ha}{(1+4Rd)}\right)^7\end{array}\right)$$

$$\Theta(15)=0$$

$$\Theta(16)=\frac{1}{20922789888000}\left(\begin{array}{l}12848000\lambda^9\left(\frac{S_h sin(\gamma)}{(1+4Rd)}\right)^8+57816000\lambda^8\left(\frac{S_h sin(\gamma)}{(1+4Rd)}\right)^7\left(\frac{Nc(1-\tilde{\varepsilon})+Nr+Ha}{(1+4Rd)}\right)\\+104504800\lambda^7\left(\frac{S_h sin(\gamma)}{(1+4Rd)}\right)^6\left(\frac{Nc(1-\tilde{\varepsilon})+Nr+Ha}{(1+4Rd)}\right)^2\\+95958800\lambda^6\left(\frac{S_h sin(\gamma)}{(1+4Rd)}\right)^5\left(\frac{Nc(1-\tilde{\varepsilon})+Nr+Ha}{(1+4Rd)}\right)^3\\+46309440\lambda^5\left(\frac{S_h sin(\gamma)}{(1+4Rd)}\right)^4\left(\frac{Nc(1-\tilde{\varepsilon})+Nr+Ha}{(1+4Rd)}\right)^4\\+10780600\lambda^4\left(\frac{S_h sin(\gamma)}{(1+4Rd)}\right)^3\left(\frac{Nc(1-\tilde{\varepsilon})+Nr+Ha}{(1+4Rd)}\right)^5\\+904082\lambda^3\left(\frac{S_h sin(\gamma)}{(1+4Rd)}\right)^2\left(\frac{Nc(1-\tilde{\varepsilon})+Nr+Ha}{(1+4Rd)}\right)^6\\+10923\lambda^2\left(\frac{S_h sin(\gamma)}{(1+4Rd)}\right)\left(\frac{Nc(1-\tilde{\varepsilon})+Nr+Ha}{(1+4Rd)}\right)^7+\lambda\left(\frac{Nc(1-\tilde{\varepsilon})+Nr+Ha}{(1+4Rd)}\right)^8\end{array}\right)$$

$$\Theta(17)=0$$

$$\Theta(18)=\frac{1}{642373705728000}\left(\begin{array}{l}496672000\lambda^{10}\left(\frac{S_h sin(\gamma)}{(1+4Rd)}\right)^9+248336000\lambda^9\left(\frac{S_h sin(\gamma)}{(1+4Rd)}\right)^8\left(\frac{Nc(1-\tilde{\varepsilon})+Nr+Ha}{(1+4Rd)}\right)\\+5109512000\lambda^8\left(\frac{S_h sin(\gamma)}{(1+4Rd)}\right)^7\left(\frac{Nc(1-\tilde{\varepsilon})+Nr+Ha}{(1+4Rd)}\right)^2\\+5537888000\lambda^7\left(\frac{S_h sin(\gamma)}{(1+4Rd)}\right)^6\left(\frac{Nc(1-\tilde{\varepsilon})+Nr+Ha}{(1+4Rd)}\right)^3\\+3348125000\lambda^6\left(\frac{S_h sin(\gamma)}{(1+4Rd)}\right)^5\left(\frac{Nc(1-\tilde{\varepsilon})+Nr+Ha}{(1+4Rd)}\right)^4\\+1091879000\lambda^5\left(\frac{S_h sin(\gamma)}{(1+4Rd)}\right)^4\left(\frac{Nc(1-\tilde{\varepsilon})+Nr+Ha}{(1+4Rd)}\right)^5\\+166874690\lambda^4\left(\frac{S_h sin(\gamma)}{(1+4Rd)}\right)^3\left(\frac{Nc(1-\tilde{\varepsilon})+Nr+Ha}{(1+4Rd)}\right)^6\\+8100380\lambda^3\left(\frac{S_h sin(\gamma)}{(1+4Rd)}\right)^2\left(\frac{Nc(1-\tilde{\varepsilon})+Nr+Ha}{(1+4Rd)}\right)^7\\+43691\lambda^2\left(\frac{S_h sin(\gamma)}{(1+4Rd)}\right)\left(\frac{Nc(1-\tilde{\varepsilon})+Nr+Ha}{(1+4Rd)}\right)^8+\lambda\left(\frac{Nc(1-\tilde{\varepsilon})+Nr+Ha}{(1+4Rd)}\right)^9\end{array}\right)$$

From the definition of DTM, we have

$$\theta(X)=\Theta(0)+\Theta(1)X+\Theta(2)X^2+\Theta(3)X^3+\Theta(4)X^4+\Theta(5)X^5+\Theta(6)X^6+...+\Theta(N)X^N \qquad (41)$$

Therefore,

$$\begin{aligned}\theta(X)=\lambda+&\frac{1}{2}\left(\lambda^2\alpha_1+\lambda\alpha_2\right)X^2+\frac{1}{24}\left(2\lambda^3\alpha_1^2+3\lambda^2\alpha_1\alpha_2+\alpha_1\alpha_2^2\right)X^4+\frac{1}{720}\left(10\lambda^4\alpha_1^3+20\lambda^3\alpha_1^2\alpha_2+11\lambda^2\alpha_1\alpha_2^2+\lambda\alpha_2^3\right)X^6+\\&\frac{1}{40320}\left(80\lambda^5\alpha_1^4+200\lambda^4\alpha_1^3\alpha_2+162\lambda^3\alpha_1^2\alpha_2^2+43\lambda^2\alpha_1\alpha_2^3+\lambda\alpha_2^4\right)X^8+\\&\frac{1}{3628800}\left(1000\lambda^6\alpha_1^5+3000\lambda^5\alpha_1^4\alpha_2+3170\lambda^4\alpha_1^3\alpha_2^2+1340\lambda^3\alpha_1^2\alpha_2^3+171\lambda^2\alpha_1\alpha_2^4+\lambda\alpha_2^5\right)X^{10}+\\&\frac{1}{476001600}\left(\begin{array}{l}17600\lambda^7\alpha_1^6+61600\lambda^6\alpha_1^5\alpha_2+80560\lambda^5\alpha_1^4\alpha_2^2+47400\lambda^4\alpha_1^3\alpha_2^3+\\11522\lambda^3\alpha_1^2\alpha_2^4+683\lambda^2\alpha_1\alpha_2^5+\lambda\alpha_2^6\end{array}\right)X^{12}+\\&\frac{1}{87178291200}\left(\begin{array}{l}418000\lambda^8\alpha_1^7+1672000\lambda^7\alpha_1^6\alpha_2+2604000\lambda^6\alpha_1^5\alpha_2^2+1960000\lambda^5\alpha_1^4\alpha_2^3\\+7087300\lambda^4\alpha_1^3\alpha_2^4+101460\lambda^3\alpha_1^2\alpha_2^5+2731\lambda^2\alpha_1\alpha_2^6+\lambda\alpha_2^7\end{array}\right)X^{14}+\\&\frac{1}{20922789888000}\left(\begin{array}{l}12848000\lambda^9\alpha_1^8+57816000\lambda^8\alpha_1^7\alpha_2+104504800\lambda^7\alpha_1^6\alpha_2^2+95958800\lambda^6\alpha_1^5\alpha_2^3+\\46309440\lambda^5\alpha_1^4\alpha_2^4+10780600\lambda^4\alpha_1^3\alpha_2^5+904082\lambda^3\alpha^2{}_1\alpha_2^6+10923\lambda^2\alpha_1\alpha_2^7+\lambda\alpha_2^8\end{array}\right)X^{16}+\\&\frac{1}{642373705728000}\left(\begin{array}{l}496672000\lambda^{10}\alpha_1^9+248336000\lambda^9\alpha_1^8\alpha_2+5109512000\lambda^8\alpha_1^7\alpha_2^2+5537888000\lambda^7\alpha_1^6\alpha_2^3\\+3348125000\lambda^6\alpha_1^5\alpha_2^4+1091879000\lambda^5\alpha_1^4\alpha_2^5+166874690\lambda^4\alpha_1^3\alpha_2^6+8100380\lambda^3\alpha_1^2\alpha_2^7+\\43691\lambda^2\alpha_1\alpha_2^8+\lambda\alpha_2^9\end{array}\right)X^{18}+...\end{aligned} \qquad (42)$$

where

$$\alpha_1 = \frac{S_h sin(\gamma)}{(1+4Rd)}, \quad \alpha_2 = \frac{Nc(1-\tilde{\varepsilon}) + Nr + Ha}{(1+4Rd)}$$

The unknown values of $\lambda$ in the Eq. (42) is found from the boundary conditions in Eq. (19b)

$$\theta(1) = \lambda + \frac{1}{2}\left(\lambda^2\alpha_1 + \lambda\alpha_2\right) + \frac{1}{24}\left(2\lambda^3\alpha_1^2 + 3\lambda^2\alpha_1\alpha_2 + \alpha_1\alpha_2^2\right) + \frac{1}{720}\left(10\lambda^4\alpha_1^3 + 20\lambda^3\alpha_1^2\alpha_2 + 11\lambda^2\alpha_1\alpha_2^2 + \lambda\alpha_2^3\right) +$$
$$\frac{1}{40320}\left(80\lambda^5\alpha_1^4 + 200\lambda^4\alpha_1^3\alpha_2 + 162\lambda^3\alpha_1^2\alpha_2^2 + 43\lambda^2\alpha_1\alpha_2^3 + \lambda\alpha_2^4\right) +$$
$$\frac{1}{3628800}\left(1000\lambda^6\alpha_1^5 + 3000\lambda^5\alpha_1^4\alpha_2 + 3170\lambda^4\alpha_1^3\alpha_2^2 + 1340\lambda^3\alpha_1^2\alpha_2^3 + 171\lambda^2\alpha_1\alpha_2^4 + \lambda\alpha_2^5\right) +$$
$$\frac{1}{476001600}\left(\begin{matrix}17600\lambda^7\alpha_1^6 + 61600\lambda^6\alpha_1^5\alpha_2 + 80560\lambda^5\alpha_1^4\alpha_2^2 + 47400\lambda^4\alpha_1^3\alpha_2^3 + \\ 11522\lambda^3\alpha_1^2\alpha_2^4 + 683\lambda^2\alpha_1\alpha_2^5 + \lambda\alpha_2^6\end{matrix}\right) +$$
$$\frac{1}{87178291200}\left(\begin{matrix}418000\lambda^8\alpha_1^7 + 1672000\lambda^7\alpha_1^6\alpha_2 + 2604000\lambda^6\alpha_1^5\alpha_2^2 + 1960000\lambda^5\alpha_1^4\alpha_2^3 \\ +7087300\lambda^4\alpha_1^3\alpha_2^4 + 101460\lambda^3\alpha_1^2\alpha_2^5 + 2731\lambda^2\alpha_1\alpha_2^6 + \lambda\alpha_2^7\end{matrix}\right) +$$
$$\frac{1}{20922789888000}\left(\begin{matrix}12848000\lambda^9\alpha_1^8 + 57816000\lambda^8\alpha_1^7\alpha_2 + 104504800\lambda^7\alpha_1^6\alpha_2^2 + 95958800\lambda^6\alpha_1^5\alpha_2^3 + \\ 46309440\lambda^5\alpha_1^4\alpha_2^4 + 10780600\lambda^4\alpha_1^3\alpha_2^5 + 904082\lambda^3\alpha^2{}_1\alpha_2^6 + 10923\lambda^2\alpha_1\alpha_2^7 + \lambda\alpha_2^8\end{matrix}\right) +$$
$$\frac{1}{642373705728000}\left(\begin{matrix}496672000\lambda^{10}\alpha_1^9 + 248336000\lambda^9\alpha_1^8\alpha_2 + 5109512000\lambda^8\alpha_1^7\alpha_2^2 + 5537888000\lambda^7\alpha_1^6\alpha_2^3 \\ +3348125000\lambda^6\alpha_1^5\alpha_2^4 + 1091879000\lambda^5\alpha_1^4\alpha_2^5 + 166874690\lambda^4\alpha_1^3\alpha_2^6 + 8100380\lambda^3\alpha_1^2\alpha_2^7 + \\ 43691\lambda^2\alpha_1\alpha_2^8 + \lambda\alpha_2^9\end{matrix}\right) + \ldots = 1$$

**Table 1.** Different values of the unknown $\lambda$ for the different values of various parameters of the model

| Rd | Nc | Nr | Ha | ε | $S_h$ | γ | $\alpha_1$ | $\alpha_2$ | λ |
|---|---|---|---|---|---|---|---|---|---|
| 0.5 | 0.6 | 0.1 | 0.7 | 0.8 | 0.1 | π/2 | 0.0333 | 0.3066 | 0.8527 |
| 0.5 | 0.6 | 0.1 | 0.7 | 0.8 | 0.3 | π/2 | 0.1000 | 0.3066 | 0.8313 |
| 0.5 | 0.6 | 0.1 | 0.7 | 0.8 | 0.6 | π/2 | 0.2000 | 0.3066 | 0.8023 |
| 0.5 | 0.6 | 0.1 | 0.7 | 0.8 | 0.9 | π/2 | 0.3000 | 0.3066 | 0.7762 |
| 0.5 | 0.1 | 0.2 | 0.6 | 0.7 | 0.3 | π/2 | 0.0714 | 0.1976 | 0.8819 |
| 0.5 | 0.3 | 0.2 | 0.6 | 0.7 | 0.3 | π/2 | 0.0714 | 0.2119 | 0.8762 |
| 0.5 | 0.6 | 0.2 | 0.6 | 0.7 | 0.3 | π/2 | 0.0714 | 0.2333 | 0.8679 |
| 0.5 | 0.9 | 0.2 | 0.6 | 0.7 | 0.3 | π/2 | 0.0714 | 0.2547 | 0.8597 |
| 0.8 | 0.5 | 0.1 | 0.3 | 0.2 | 0.7 | π/2 | 0.3181 | 0.3636 | 0.7549 |
| 0.8 | 0.5 | 0.3 | 0.3 | 0.2 | 0.7 | π/2 | 0.3181 | 0.4545 | 0.7291 |
| 0.8 | 0.5 | 0.6 | 0.3 | 0.2 | 0.7 | π/2 | 0.3181 | 0.5909 | 0.6929 |
| 0.8 | 0.5 | 0.9 | 0.3 | 0.2 | 0.7 | π/2 | 0.3181 | 0.7272 | 0.6592 |
| 0.6 | 0.1 | 0.7 | 0.1 | 0.4 | 0.5 | π/2 | 0.1470 | 0.2529 | 0.8360 |
| 0.6 | 0.1 | 0.7 | 0.3 | 0.4 | 0.5 | π/2 | 0.1470 | 0.3117 | 0.8155 |
| 0.6 | 0.1 | 0.7 | 0.6 | 0.4 | 0.5 | π/2 | 0.1470 | 0.4000 | 0.7862 |
| 0.6 | 0.1 | 0.7 | 0.9 | 0.4 | 0.5 | π/2 | 0.1470 | 0.4882 | 0.7584 |

## 5. RESULTS AND DISCUSSION

The approximate analytical solutions are coded in MATLAB, and the parametric and sensitivity analyses are carried out using the codes. However, before the parametric and sensitivity analyses, the results of the developed solutions are verified with the results of numerical method (NM) using fourth-order shown in Table 2. The reduced lower marginal differences between the results of the DTM and that of the HAM confirms the higher level of accuracy of the DTM than HAM, as shown in the Table 2.

**Table 2.** Comparison of results.

| *The results of HAM, DTM and Numerical methods for $\vartheta(X)$ for Rd = 0.5, $\varepsilon$ = 0.1, $S_h$= 0.4, Nc = 0.3, Nr = 0.2, Ha = 0.1, λ=0* | | | | | |
|---|---|---|---|---|---|
| | | | $\vartheta(X)$ | | |
| *X* | NUM | HAM | DTM (present work) | Error of DTM | Error of HAM |
| 0.00 | 0.863499231 | 0.863499664 | 0.863499158 | 0.000000073 | 0.000000433 |
| 0.20 | 0.868776261 | 0.868776709 | 0.868776195 | 0.000000066 | 0.000000448 |
| 0.40 | 0.884696500 | 0.884696967 | 0.884696438 | 0.000000062 | 0.000000467 |
| 0.60 | 0.911530658 | 0.911531120 | 0.911530606 | 0.000000052 | 0.000000462 |
| 0.80 | 0.949741203 | 0.949741555 | 0.949741166 | 0.000000037 | 0.000000352 |
| 1.00 | 1.000000000 | 1.000000000 | 1.000000000 | 0.000000000 | 0.000000000 |

The impacts of convective, radiative, magnetic, and porous parameters on the adimensional temperature distribution, heat transfer at the fin base, and thermal efficiency of the fin are presented in Figs. 3-7. It is shown in the figures that when the inclination of fin, convective, radiative, magnetic, and porous parameters increase, the adimensional fin temperature decreases. It could be stated that low values of inclination of fin, convective, radiative, magnetic, and porous parameters favour thermal performance or efficiency of the fin. Therefore, the porous fin is more efficient and effective for relatively low values of fin inclination, convective, radiative, magnetic, and porous parameters.

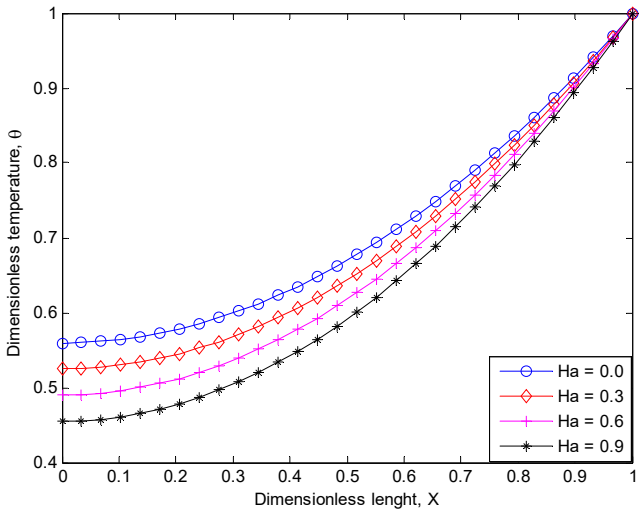


**Figure 4.** Effects of Hartmann number on the adimensional temperature distribution in the fin.

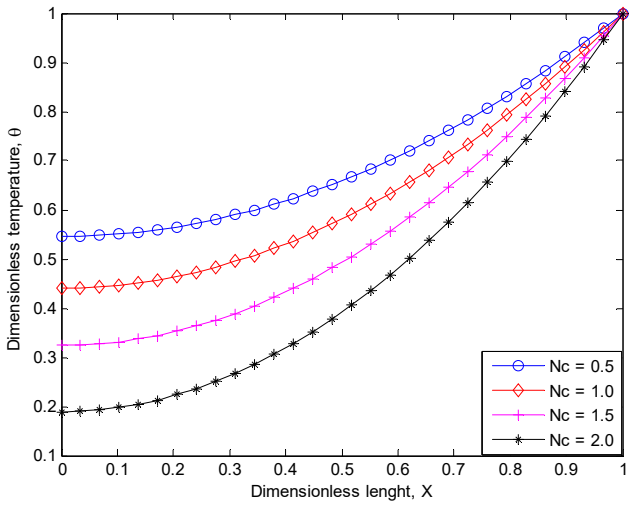


**Figure 5.** Effects of convective parameter on the adimensional temperature distribution in the fin.

Fig. 3 shows the effect of inclination of fin on the dimensionless temperature distribution in the fin. The figure shows that as the inclination of fin increases (the vertical distance of the prime surface increases), the adimensional temperature distribution in the fin decreases (the fin thermal profile falls, as shown in the figure). The reduction in the local temperature of the fin as the inclination of the fin increases is due to increase in the driving force for convection and buoyancy of the working fluid around the extended surface.

Fig. 4 illustrates the effect of Hartman number (magnetic field parameter) on the adimensional temperature distribution in the fin. The temperature in the fin decreases as the magnetic parameter increases. Increase in the magnetic parameter or Hartmann number causes increase in Lorentz force which provides resistive force that opposes motion of the working fluid around the fin and consequently decreases the temperature of the fin.

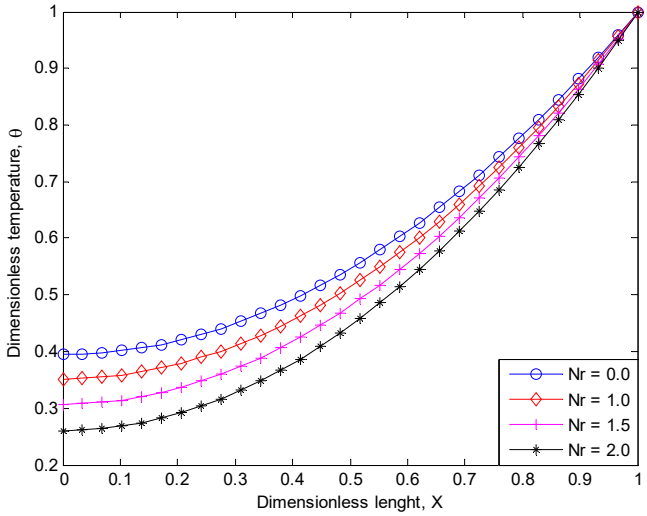


**Figure 6.** Effects of radiative parameter on the adimensional temperature distribution in the fin.

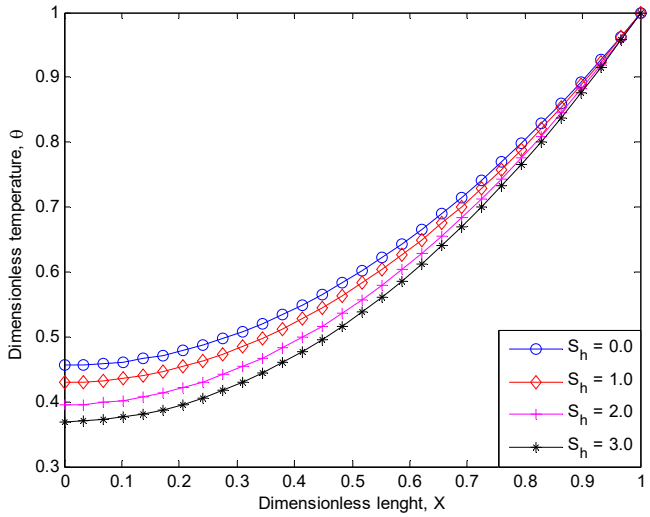


**Figure 7.** Effects of porous parameter on the adimensional temperature distribution in the fin.

Fig. 5 and 6 presents the influences of convective and radiative parameters on the dimensionless temperature distribution in the fin, respectively. The figures show that as the convective and radiative parameters increase, the adimensional local temperature in the fin decreases as the convective and radiative parameters. This is because, as the convective and radiative parameters increase, the effects of convective and radiative heat transfer on the fin surface increase, thereby, more heat is loss through the surface of the fin. As a consequent, surface temperature of the fin drops (the fin thermal profile falls) and the rate of heat transfer from the fin increases as the convective and radiative parameters increase. It should be noted that the low value of the convective and radiative parameters, *Nc* and *Nr* implies a relatively thick and short fin of very high thermal conductivity, while a high value of the convective and radiative parameters indicates a relatively thin and long fin of a very low thermal conductivity. Therefore, the thermal efficiency of the fin is favoured at low values of convective and radiative parameters, i.e. a relatively thick and short fin with a high thermal conductivity.

Fig. 7 shows the impact of porous parameter on the dimensionless temperature distribution in the fin. The figure shows that as the porous parameter (Rayleigh number) increases, the adimensional temperature in the fin decreases. The fin temperature decreases as the porosity parameter increases because of the increase in the permeability of fin which makes the working fluid to infiltrate more through the pores of the fin and increase the buoyancy force effect. Consequently, more heat is taken away from the surface of the fin as the temperature falls more. This establishes that the thermal efficiency of the fin increases as the Rayleigh number is enlarged.

From the above parametric studies, it could be clearly stated that the fin is more efficient and effective for relatively low values of inclination of fin, convective, radiative, magnetic, and porous parameters. However, these values of these parameters should be properly selected to avoid thermal stability in the fin.

## 6. CONCLUSION

This work has demonstrated a comparative application of homotopy analysis and differential transformation methods to study the thermal performance of magnetohydrodynamic convective-radiative porous fin with temperature-invariant thermal conductivity. Also, the effects of other parameters of the thermal model parameters on the heat transfer behaviour of the extended surface are analytically investigated using the methods. Therefore, the present work will help in the proper analysis of fin and in the design of passive heat enhancement for thermal and electronic systems.

### Nomenclature

A cross sectional area, $A_b$ porous fin base area
$c_p$ specific heat capacity of the fluid passing through porous fin,
h heat transfer coefficient
$k_{eff}$ effective thermal conductivity
L fin length
Ra Rayleigh number
Rd Radiation number
t fin thickness of the fin
$T_b$ temperature at the fin base
T fin temperature
$T_a$ ambient temperature, K
u fluid average velocity
x axial length of the fin
X dimensionless fin length
w width of the fin width

### Greek

θ dimensionless temperature
ε porosity or void ratio
υ kinematic viscosity
ρ fluid density of the fluid

### References

[1] S. Kiwan and M. A. Al-Nimr, "Using Porous Fins for Heat Transfer Enhancement," Journal of Heat Transfer, 123(2000), 790-795.

[2] L. Gong, Y. Li, Z. Bai, and M. Xu, "Thermal performance of micro-channel heat sink with metallic porous/solid compound fin design," Applied Thermal Engineering, 137(2018), 288-295.

[3] H. M. Ali, M. J. Ashraf, A. Giovannelli, M. Irfan, T. B. Irshad, H. M. Hamid, et al., "Thermal management of electronics: An experimental analysis of triangular, rectangular and circular pin-fin heat sinks for various PCMs," International Journal of Heat and Mass Transfer, 123(2018), 272-284.

[4] M. O. Seyfolah Saedodin, "Temperature distribution in porous fins in natural convection condition," Journal of American Science, 7, 2011.

[5] G. A. Oguntala, R. A. Abd-Alhameed, G. M. Sobamowo, and N. Eya, "Effects of particles deposition on thermal performance of a convective-radiative heat sink porous fin of an electronic component," Thermal Science and Engineering Progress, 6(2018), 177-185.

[6] M. G. Sobamowo, O. M. Kamiyo and O. A. Adeleye. Thermal performance analysis of a natural convection porous fin with temperature-dependent thermal conductivity and internal heat generation. Thermal Science and Engineering Progress, 1(2017), 39-52.

[7] S. Mosayebidorcheh, M. Farzinpoor, and D. D. Ganji, "Transient thermal analysis of longitudinal fins with internal heat generation considering temperature-dependent properties and different fin profiles," Energy Conversion and Management, 86(2014), 365-370.

[8] S.-M. Kim and I. Mudawar, "Analytical heat diffusion models for different micro-channel heat sink cross-sectional geometries," International Journal of Heat and Mass Transfer, 53(2010), 4002-4016.

[9] A. Moradi, T. Hayat, and A. Alsaedi, "Convection-radiation thermal analysis of triangular porous fins with temperature-dependent thermal conductivity by DTM," Energy Conversion and Management, 77(2014), 70-77.

[10] G. Oguntala, R. Abd-Alhameed, and G. Sobamowo, "On the effect of magnetic field on thermal performance of convective-radiative fin with temperature-dependent thermal conductivity," Karbala International Journal of Modern Science, 4(2018), 1-11.

[11] Z. M. Wan, G. Q. Guo, K. L. Su, Z. K. Tu, and W. Liu, "Experimental analysis of flow and heat transfer in a miniature porous heat sink for high heat flux application," International Journal of Heat and Mass Transfer, 55(2012), 4437-4441.

[12] P. Naphon, S. Klangchart, and S. Wongwises, "Numerical investigation on the heat transfer and flow in the mini-fin heat sink for CPU," International Communications in Heat and Mass Transfer, 36(2009), 834-840.

[13] [13] G. Oguntala, R. Abd-Alhameed, G. Sobamowo, and I. Danjuma, "Performance, Thermal Stability and Optimum Design Analyses of Rectangular Fin with Temperature-Dependent Thermal Properties and Internal Heat Generation," Journal of Computational Applied Mechanics, 49(2018), 37-43.

[14] M. G. Sobamowo, "Thermal analysis of longitudinal fin with temperature-dependent properties and internal heat generation using Galerkin's method of weighted residual," Applied Thermal Engineering, 99(2016), 1316-1330.

[15] H. R. Seyf and M. Feizbakhshi, "Computational analysis of nanofluid effects on convective heat transfer enhancement of micro-pin-fin heat sinks," International Journal of Thermal Sciences, 58(2012), 168-179.

[16] S. A. Fazeli, S. M. Hosseini Hashemi, H. Zirakzadeh, and M. Ashjaee, "Experimental and numerical investigation of heat transfer in a miniature heat sink utilizing silica nanofluid," Superlattices and Microstructures, 1(2012), 247-264.

[17] S. J. Liao. Beyond perturbation: introduction to the homotopy analysis method. Boca Raton (FL): Chapman & Hall/CRC Press; 2003.